Interfacial Properties of N_{TAIL}, an Intrinsically Disordered Protein

AN-01

Issues:

- Disordered proteins, like proteins involved in neurodegenerative diseases (Alzheimer, Parkinson…) are devoid of stable secondary and tertiary structure under physiological conditions.
- These proteins can form protein aggregates, may be triggered by the interaction with cellular membranes.
- There is a need for more information on the interfacial behaviour of disordered proteins and comparison with globular/ordered proteins.

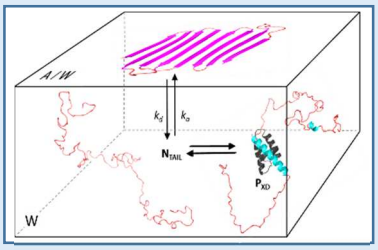

Apparatus:

Tracker™ Drop Tensiometer

Introduction

Proteins are essential for the organism, they participate in every process within the living cell. They play crucial structural and functional roles. If their function is impaired, this can lead to various pathologies. These dysfunctions are often associated with gene mutations leading to inactive or noncorrectly folded proteins/enzymes. This usually applies to globular proteins with well-defined 3D structure and function(s) associated with this structure. The figure below highlights the convontional proteins dogma dictating that the structure of proteins determines their function, so far accepted but now questionned:

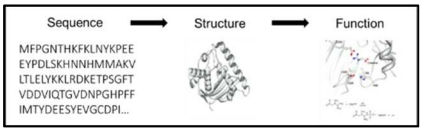

But there is an increasing evidence that intrinsically disordered proteins (IDPs) or intrinsically disordered protein regions are highly represented among proteins [1]. It is not because a protein is disordered that it has no biological function.

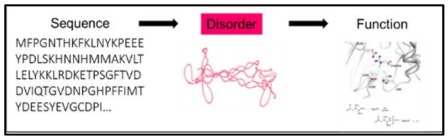

On the contrary, they have a widespread role in biological processes especially in eukarya, such as transcription, cell cycle, mitosis, apoptosis etc… [2]. New concepts have emerged to describe and possibly explain some protein misfolding disorders such as neurodegenerative diseases. Indeed, the aggregation of IDPs into amyloid fibrils is directly associated with the onset and progression of these pathological disorders. For instance, Alzheimer's and Parkinson's diseases are tightly associated with the aggregation of otherwise soluble IDPs that form protein deposits in the brain of patients and lead to neuronal death [3-7]. This figure below shows the concept of misfolded proteins forming aggregates in the case of neurodegenerative diseases:

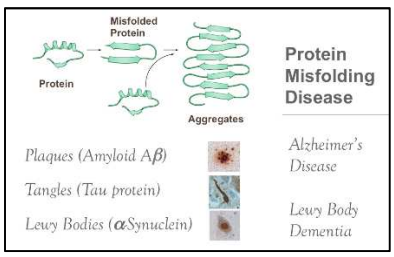

In that context, it is important to better understand the key factors that can trigger the folding and aggregation of IDPs. IDPs are functional proteins that are devoid of stable secondary and tertiary structure under physiological conditions of pH and salinity in

the absence of a partner/ligand [2, 8-10]. They thus exist as dynamic ensembles of interconverting conformers and differ from structured globular proteins at several levels, including amino acid composition, sequence complexity, hydropathy, charge, and flexibility. IDPS are enriched in polar/charged residues. Because of this enrichment, IDPs are characterized by a hydration significantly higher than that of ordered proteins [11]. As such, IDPs can reasonably be expected to exhibit a distinct behavior not only in bulk but also at air/water (A/W) and lipid/water interfaces. There is a need for more information on the interfacial behavior of IDPs and comparison with globular proteins, so we investigated the study of interfacial properties of a model IDP, the intrinsically disordered C-terminal domain of the Hendra virus (HeV) nucleoprotein (N_{TAIL}), a protein responsible for the encapsidation of the viral genome [12, 13]. HeV N_{TAIL} is a disordered protein domain of 140 residues and 15.3 kDa that has been well characterized by various biophysical approaches [14-16].In this study, we compared the behavior of HeV N_{TAIL} at the air-water interface, in the absence and presence of phospholipids, with that of lysozyme using the dynamic drop tensiometer Tracker™.

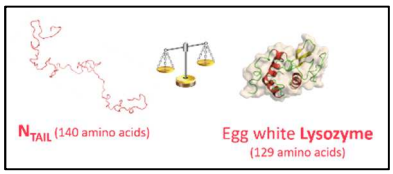

Lysozyme served as a model of folded globular protein having a molecular mass (14.3 kDa) close to that of HeV N_{TAIL}.

Material

An automated drop tensiometer is an apparatus allowing the measure of the surface tension between two immiscible constituents (oil/water, air/water, …).

A drop/bubble is generated at the end of a syringe needle. The drop/bubble is held thanks to the surface tension forces and is deformed due to gravity. The analysis of the shape of the drop gives us the access to the surface tension.

This analysis is done with a CCD Camera and an algorithm allowing to do up to 120 measures/sec. The apparatus is equipped with a motor for creating the drop, to keep the volume of the drop constant and to apply mechanical stresses, for example of the sinusoidal type.

The monitoring of the surface tension as a function of time gives us indications on the time that the surfactant comes to the surface and on the effectiveness of the surfactant to lower the surface tension (the lower the tension is the more the energy to disperse the two phases will be low). The following example shows a tension curve as a function of time (adsorption kinetics) for an air bubble in the presence of surfactants:

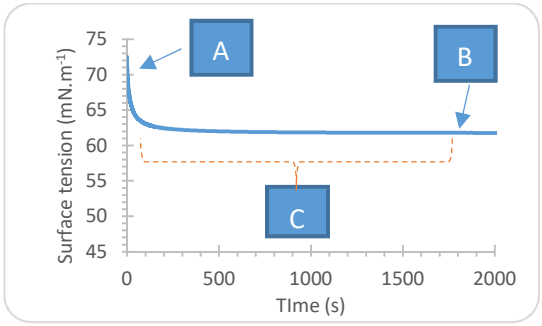

A : Initial surface tension, the surface is virgin (without surfactants)

B : Equilibrium surface tension, the concentration of surfactant is stable (the surfactants are on the surface of the air bubble).

C : Time for the surfactant to reach the surface (adsorption kinetic).

The sinusoidal type constraints give us indications on the behavior of the surfactant on the surface.

These (dilatational) constraints make it possible to vary the surfactant concentration at the surface by increasing and decreasing the area of the bubble. A variation of the surface concentration causes a variation of the surface tension.

Sinusoidal oscillation of the bubble

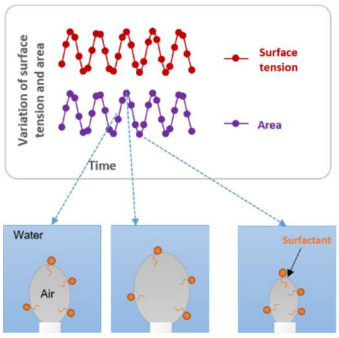

On the previous diagram we can see the change of surface concentration according to the area of the drop and the effect on the surface tension, there are always four surfactants on a larger or smaller surface.

These variations of area and tension allow us to calculate the viscoelastic module.

$$E = \frac{d\gamma}{dlnA} \qquad (1)$$

With:

E= viscoelastic modulus (N.m^{-1})
γ=Surface tension (N.m^{-1})
A= area (m^2).
This module can also be broken down into an elastic part E', a viscous part E'' and a phase shift.
We speak of an elastic surface when the adsorbed surfactants do not desorb (do not leave the surface) or very little according to the sinusoidal stresses.

The surface viscosity as well as the phase shift occur rather when there is an exchange between the surface of the bubble and the medium.

The figure below allows to figure out the viscoelastic modulus:

Elastic case:

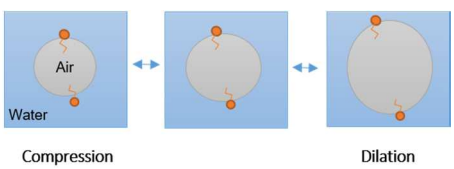

Little exchange between the surface and the environment.

Viscoelastic case:

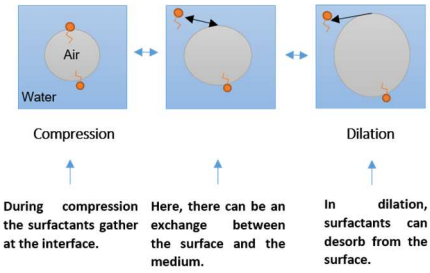

Depending on the oscillation frequency of this bubble, more elastic or more viscous behaviors can be observed. To be elastic, it is sufficient to choose a faster oscillation frequency than the exchange of the surfactant with the surface and the medium.

The surface pressure Π can be measured thanks to the surface tension (in N.m^{-1}):

$$\Pi = \gamma_0 - \gamma \qquad (2)$$

with γ_0 the surface tension without surfactant (for example equaled to 72.7 mN.m^{-1} at the air/water interface or around 30 mN.m^{-1} at the oil/water interface) and γ the surface tension in presence of surfactant.

Variations in the surface dilational modulus E as a function of surface pressure Π can be fitted using a 2D solution treatment. Surface pressure is given by a first-order surface equation of state based on Frumkin-Lucassen's isotherm and including terms for entropy and enthalpy of surface mixing of solvent and surfactant with nonequal molecular area [17]:

$$\Pi = \frac{RT}{\omega_1}\left[-\ln\left(1-\frac{\Gamma}{\Gamma_{inf}}\right)-\left(1-\frac{1}{S}\right)\frac{\Gamma}{\Gamma_{inf}}-\frac{H}{RT}\left(\frac{\Gamma}{\Gamma_{inf}}\right)^2\right] \qquad (3)$$

With ω_1 is the molecular area of the solvent (water), S is a size factor defined as the ratio of the molecular area of surfactant or solute (protein or egg PC in this study) to that of the solvent, H is the molar enthalpy of mixing at infinite dilution, Γ is the surface concentration of surfactant, Γ_{inf} is the maximum or saturation surface concentration of surfactant, R is the ideal gas constant, and T is the temperature. The dilational modulus E is given by the following equation [18, 19]:

$$E = \frac{RT}{\omega_1}\left[\frac{\frac{\Gamma}{\Gamma_{inf}}}{1-\frac{\Gamma}{\Gamma_{inf}}} - \left(1-\frac{1}{S}\right)\frac{\Gamma}{\Gamma_{inf}} - \frac{2H}{RT}\left(\frac{\Gamma}{\Gamma_{inf}}\right)^2\right] \quad (4)$$

Experimental protocol and results

Our study was conducted in two parts :

1) The adsorption of N_{TAIL}, Lysozyme and eggPC at the air/water interface.
2) The adsorption of N_{TAIL} and lysozyme onto an eggPC film previously adsorbed around an air bubble.

In this latter case, we compared the interfacial behaviors of the two proteins onto a monolayer of egg PC because this phospholipid is the major component found in physiological cellular membranes (among others such as proteins and other minor types of phospholipids).

Adsorption of N_{TAIL}, lysozyme, and eggPC at the Air/Water interface.

We compared the adsorption of N_{TAIL}, lysozyme, and the phospholipid lecithin from egg yolk (also named eggPC) at the surface of an air bubble. We can see below a schematic representation of the type of experiment (Fig (A)):

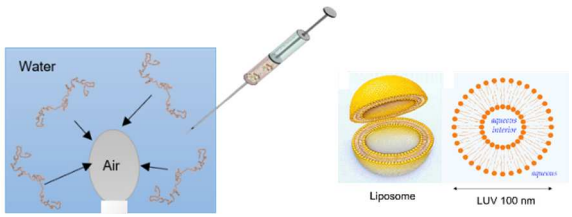

Fig. 1: Schématic representations of (A) an air bubble at the end of a syringe needle immerged in a buffer with an injection of proteins and (B) a large unilamellar vesicle of phopholipids of 100 nm corresponding to a liposome.

We measured changes in surface pressure after injection of the protein (80 nM) or phospholipids (0.05% w/v final concentration) in the bulk phase. Phospholipids were injected in the form of LUVs (large unilamellar vesicles) of 100 nm of diameter (Fig. 1B). The bulk buffer was 10 mM Tris/HCl (pH 7.0), 100 mM NaCl, and 21 mM $CaCl_2$.

In Fig. 2, we can see the surface pressure monitored for the two proteins and eggPC as the function of time allowing to have information on their adsorption kinetics.

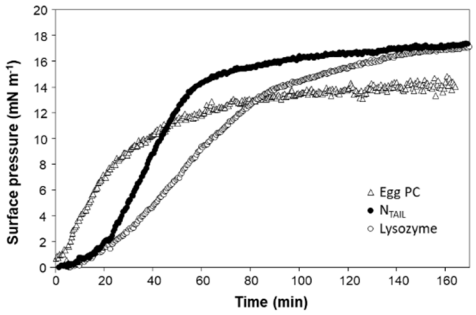

Fig. 2: Adsorption of N_{TAIL}, lysozyme and phospholipids (egg PC) at the air-water interface, measured using the Tracker™ drop tensiometer.

The increase in the surface pressure was faster with eggPC than with N_{TAIL} and lysozyme, which both featured a lag phase of ≈15 min before the surface pressure increase has reached its maximum rate. Subsequently, N_{TAIL} then displayed a faster adsorption kinetics compared to lysozyme. The surface pressures that were reached at equilibrium were 14.1 ± 0.3 $mN.m^{-1}$ for egg PC, 17.5 ± 0.9 $mN.m^{-1}$ for N_{TAIL}, and 17.1 ± 0.3 mN m^{-1} for lysozyme. The value obtained with lysozyme is identical to the surface pressure previously recorded with native lysozyme by Desfougères *et al.* [20], although the protein bulk concentration used in that previous study (0.1 $mg.L^{-1}$ or 7 mM) was 87 times higher than the concentration we used here. The value obtained with eggPC is similar to the equilibrium surface pressure previously recorded by Mitsche *et al.* [21] using the same drop tensiometer Tracker™.

The mechanical response to compression/dilation of the protein and egg PC layers at the A/W interface was measured simultaneously to adsorption by using sinusoidal oscillations of the air-bubble volume and thus of interfacial area A ($\Delta A/A = 0.25$ at a frequency of 0.2 Hz). The surface dilational modulus E (Fig. 3 (A))

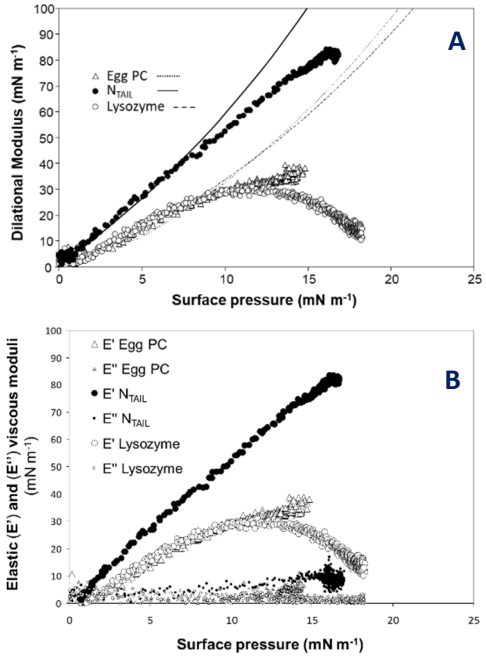

Fig. 3: (A) Interfacial rheometry. Variation of the dilational modulus with surface pressure for N_{TAIL}, lysozyme and phospholipids (egg PC) at the air-water interface. (B) Corresponding elastic (E') and viscous moduli (E'') of the dilational modulus as the function of the surface pressure.

and its elastic (E') and viscous (E'') components (Fig. 3(B)) were continuously determined for both proteins and egg PC, and were plotted as a function of surface pressure Π. The dilational modulus recorded for lysozyme as a function of the surface pressure showed a bell-shaped variation with a maximum value of 30 $mN.m^{-1}$ at a surface pressure of ≈ 12 $mN.m^{-1}$. Before the inflection, the dilational modulus of lysozyme was similar to that of phospholipids (Fig. 3(A)). The lysozyme layer at the Air/Water interface showed a quasi-pure elastic behavior as indicated by the E''/E' ratio, which was 0.071 at 15 $mN.m^{-1}$ (Fig. 3(B)). This indicates no shift between surface area of the bubble and surface tension variations when the frequency of sinusoidal oscillations was 0.2 Hz. We also performed dilational rheometry experiments at various frequencies from 0.1 to 1 Hz, and always observed a very low phase angle for lysozyme (data not shown). The dilational modulus observed with N_{TAIL} was much higher, reaching values of ≈ 80 $mN.m^{-1}$, and it showed a linear increase with surface pressure up to 15 $mN.m^{-1}$ (Fig. 3 (A)). This indicates that N_{TAIL} molecules have a much stronger interaction between each other compared to lysozyme and egg PC molecules. Compared to lysozyme, the N_{TAIL} layer at the Air/Water interface also showed a viscoelastic behavior with a significant viscous modulus and an E''/E' ratio of 0.12 at 15 $mN.m^{-1}$. The E(Π) data points were then fitted with a 2D solution treatment (see Eqs. 3 and 4 in Materials and Methods) to provide a description of E(Π) variations in the elastic range where E is dominated by the equation of state, i.e., for values of Π < 10 $mN.m^{-1}$ [19]. A good fit was obtained for surface pressures below 8 $mN.m^{-1}$ for N_{TAIL}, lysozyme, and egg PC (Fig. 3(A)). Above this surface pressure, deviations occur that probably reflect molecular rearrangements of the surfactants at the Air/Water interface. This treatment allowed estimating the interaction parameter H corresponding to the molar enthalpy of mixing at the surface, and the size factor S that corresponds to the solvent molecule equivalents displaced by the surfactant (protein or eggPC) upon adsorption at the A/W interface. Negative values for H represent attractive forces between surfactants and solvent (water) and repulsive forces between surfactants at interfaces, whereas positive values indicate attractive interactions between the surfactant molecules at the interface [17]. We observed this situation in all cases, but these interactions were stronger for N_{TAIL} (H ≈ 0.65 RT) than for lysozyme (H ≈ 0.2 RT), whereas an intermediate value was obtained for egg PC (Table 1).

Surfactant/Solute	H/RT	S
Egg PC	0.5	5.5
Lysozyme	0.2	37
N_{TAIL}	0.65	120

Table 1: Parameter values used for fitting experimental data of dilational modulus variations versus surface pressure with the 2D Solution Model.

Based on S values, N_{TAIL} (S ≈ 120) displaces more solvent molecules from the interface than lysozyme (S = 37) and egg PC (S = 5.5). The initial variation of

the dilational modulus with surface pressure ($\Delta E/\Delta\Pi$) was also found to be higher with N_{TAIL} (5.46) than with lysozyme (2.84) and eggPC (2.64), which supports stronger interactions between N_{TAIL} molecules at the interface.

Discussion and conclusions

Compared to lysozyme, the intrinsically disordered protein N_{TAIL} presents a significant surface activity and adsorbs rapidly at the Air/Water interface to form a highly viscoelastic film. The formation of this film, strong intermolecular interactions, and significant viscosity (Fig. 3(B)) probably results from the fact that the N_{TAIL} polypeptide is totally spread at the Air/Water interface.

A pure elastic behavior and also fewer interactions between the molecules were observed for the lysozyme. This suggests that lysozyme stayed at the Air/Water interface, without deformation or exchange with the water.

Protein adsorptions in the presence of egg PC were also tested, but additional changes in surface pressure induced by the protein were weak and hardly interpretable (data not shown), probably because the surface pressure reached after eggPC injection was close to the critical surface pressure of penetration of both proteins. Dilational rheometry further confirmed that the interfacial properties were mainly controlled by phospholipids under these conditions (data not shown).

Apart from fundamental considerations, the properties of IDPs at interfaces may be useful for engineering protein layers at various interfaces (i.e., stabilization of emulsions, blocking the adsorption of other proteins/enzymes [22].

The association of IDPs with interfaces and/or membranes may therefore lead to various applications.

To conclude, surface tension measurements allow us to have information on the adsorption kinetics and the effectiveness of the surfactant in lowering the surface tension. Measurements of the viscoelastic module are complementary because they make it possible to "map" the surface and especially to make assumptions about its organization.

To keep more information about these results, see the publication BIOPHYSICAL *Journal* Volume 113, Issue12 p2723–2735, 19 December 2017 DOI: 10.1016/j.bpj.2017.10.010

References:

1. Dunker, A.K., et al., *What's in a name? Why these proteins are intrinsically disordered: Why these proteins are intrinsically disordered.* Intrinsically Disord Proteins, 2013. **1**(1): p. e24157.
2. Wright, P.E. and H.J. Dyson, *Intrinsically unstructured proteins: re-assessing the protein structure-function paradigm.* J Mol Biol, 1999. **293**(2): p. 321-31.
3. Fink, A.L., *The aggregation and fibrillation of alpha-synuclein.* Acc Chem Res, 2006. **39**(9): p. 628-34.
4. Galvagnion, C., et al., *Chemical properties of lipids strongly affect the kinetics of the membrane-induced aggregation of alpha-synuclein.* Proc Natl Acad Sci U S A, 2016. **113**(26): p. 7065-70.
5. Galvagnion, C., et al., *Lipid vesicles trigger alpha-synuclein aggregation by stimulating primary nucleation.* Nat Chem Biol, 2015. **11**(3): p. 229-34.
6. Jiang, D., et al., *A kinetic model for beta-amyloid adsorption at the air/solution interface and its implication to the beta-amyloid aggregation process.* J Phys Chem B, 2009. **113**(10): p. 3160-8.
7. Jones, E.M., et al., *Interaction of tau protein with model lipid membranes induces tau structural compaction and membrane disruption.* Biochemistry, 2012. **51**(12): p. 2539-50.

8. Dunker, A.K., et al., *Intrinsically disordered protein.* J Mol Graph Model, 2001. **19**(1): p. 26-59.
9. Habchi, J., et al., *Introducing protein intrinsic disorder.* Chem Rev, 2014. **114**(13): p. 6561-88.
10. Uversky, V.N., *Natively unfolded proteins: a point where biology waits for physics.* Protein Sci, 2002. **11**(4): p. 739-56.
11. Bokor, M., et al., *NMR relaxation studies on the hydrate layer of intrinsically unstructured proteins.* Biophys J, 2005. **88**(3): p. 2030-7.
12. Habchi, J. and S. Longhi, *Structural disorder within paramyxovirus nucleoproteins and phosphoproteins.* Mol Biosyst, 2012. **8**(1): p. 69-81.
13. Longhi, S., et al., *How order and disorder within paramyxoviral nucleoproteins and phosphoproteins orchestrate the molecular interplay of transcription and replication.* Cell Mol Life Sci, 2017. **74**(17): p. 3091-3118.
14. Communie, G., et al., *Atomic resolution description of the interaction between the nucleoprotein and phosphoprotein of Hendra virus.* PLoS Pathog, 2013. **9**(9): p. e1003631.
15. Habchi, J., et al., *Structural disorder within Henipavirus nucleoprotein and phosphoprotein: from predictions to experimental assessment.* PLoS One, 2010. **5**(7): p. e11684.
16. Martinho, M., et al., *Assessing induced folding within the intrinsically disordered C-terminal domain of the Henipavirus nucleoproteins by site-directed spin labeling EPR spectroscopy.* J Biomol Struct Dyn, 2013. **31**(5): p. 453-71.
17. Lucassen-Reynders, E.H., A. Cagna, and J. Lucassen, *Gibbs elasticity, surface dilational modulus and diffusional relaxation in nonionic surfactant monolayers.* Colloids and Surfaces A: Physicochemical and Engineering Aspects, 2001. **186**(1): p. 63-72.
18. Lucassen-Reynders, E., A. Cagna, and J. Lucassen, *Gibbs elasticity, surface dilational modulus and diffusional relaxation in nonionic surfactant monolayers.* Colloids and Surfaces A: Physicochemical and Engineering Aspects, 2001. **186**(1): p. 63-72.
19. Benjamins, J., J. Lyklema, and E.H. Lucassen-Reynders, *Compression/expansion rheology of oil/water interfaces with adsorbed proteins. Comparison with the air/water surface.* Langmuir, 2006. **22**(14): p. 6181-8.
20. Desfougeres, Y., et al., *Strong improvement of interfacial properties can result from slight structural modifications of proteins: the case of native and dry-heated lysozyme.* Langmuir, 2011. **27**(24): p. 14947-57.
21. Mitsche, M.A., L. Wang, and D.M. Small, *Adsorption of egg phosphatidylcholine to an air/water and triolein/water bubble interface: use of the 2-dimensional phase rule to estimate the surface composition of a phospholipid/triolein/water surface as a function of surface pressure.* J Phys Chem B, 2010. **114**(9): p. 3276-84.
22. Scheuble, N., et al., *Blocking Gastric Lipase Adsorption and Displacement Processes with Viscoelastic Biopolymer Adsorption Layers.* Biomacromolecules, 2016. **17**(10): p. 3328-3337.